Journal of Power Sources 205 (2012) 474–478

Contents lists available at SciVerse ScienceDirect

Journal of Power Sources

journal homepage: www.elsevier.com/locate/jpowsour

Short communication

Nano-carbon/sulfur composite cathode materials with carbon nanofiber as electrical conductor for advanced secondary lithium/sulfur cells

Mumin Rao [a,b,1], Xiangyun Song [b], Elton J. Cairns [a,b,*]

[a] Department of Chemical and Biomolecular Engineering, University of California, Berkeley, CA 94720, USA
[b] Environmental Energy Technologies Division, Lawrence Berkeley National Laboratory, Berkeley, CA 94720, USA

ARTICLE INFO

Article history:
Received 29 October 2011
Received in revised form
12 December 2011
Accepted 1 January 2012
Available online 9 January 2012

Keywords:
Lithium/sulfur cell
Carbon nanofiber
Carbon particle
Nanocomposite
Lithium battery

ABSTRACT

A carbon particle supported sulfur (C–S) composite cathode material was prepared by a chemical deposition method in an aqueous solution. The performance of the C–S cathode material with carbon particles (CP) and carbon nanofibers (CNFs) as electrical conductors and CMC + SBR as binder was evaluated in Li/S cells using cyclic voltammetry, constant current cycling, and electrochemical impedance spectroscopy. The C–S material and the electrodes were examined by scanning electron microscopy. It is found that the C–S cathode with CNFs shows improvement of not only discharge capacity but also cycling durability. It exhibits an initial discharge capacity of 1200 mAh g^{-1}, or 72% of theoretical, and retains 668 mAh g^{-1}, or 40% of the sulfur theoretical capacity after 50 cycles. The C–S electrode with CNFs has a three-dimensional network structure with regular pores, which can suppress the agglomeration of sulfur or lithium sulfide. Thus, the cell performance is improved.

1. Introduction

Lithium cells are very attractive for clean energy storage electric vehicles (EVs) and hybrid electric vehicles (HEVs) due to their high specific energy and good cycle life [1–4]. However, popular cathode materials such as $LiCoO_2$, $LiMnO_2$ and $LiFePO_4$ have low specific capacities compared to what is needed for EV applications. Sulfur is a promising electrode material for high-specific-energy lithium cells with a theoretical specific capacity of 1675 mAh g^{-1} and theoretical specific energy (when paired with a Li metal electrode) of 2600 Wh kg^{-1} [5–10]. However, the highly insulating nature of sulfur and the high solubility of lithium polysulfides as intermediate products generated during the discharge process in traditional organic electrolytes have limited its use [11–14]. One of the ways to solve these problems is to use a carbon support to prepare a carbon/sulfur composite to increase the electronic conductivity of the sulfur cathode [15–18]. In addition, the ionic conductivity of the sulfur cathode can be enhanced by incorporation of an ionic conductor into the electrode matrix [19,20].

In this work, we report a simple chemical deposition method to synthesize a carbon particle supported core–shell composite cathode material and use carbon nanofibers (CNFs) and carbon particles (CP) as additional electronic conductors for the sulfur cathode. The conductivity of the C–S composite material is improved using carbon particles as a support for sulfur, and using CNFs as an additional electronic conductor. Cyclic voltammograms, electrochemical impedance spectroscopy, SEM studies of morphological changes of the cathodes, and charge–discharge performance of the C–S composites with CNFs and CP were used to investigate and characterize the sulfur electrodes.

2. Experimental procedures

2.1. Preparation of carbon–sulfur composites

C–S composites were prepared by a chemical deposition method as discussed in our previous report [21,22]. Carbon particles were purchased from Sigma–Aldrich. 0.58 g sodium sulfide (Na_2S, Aldrich) was added into a flask that has been filled with 20 ml distilled water to form a Na_2S solution, then 0.72 g elemental sulfur was suspended in Na_2S solution and stirred with a magnetic stirrer for about 2 h at room temperature to obtain a sodium polysulfide (Na_2S_x) solution. The reaction formula is as follows:

$$Na_2S + (x-1)S \rightarrow Na_2S_x$$

0.18 g Carbon particles were dispersed in 100 ml distilled water and sonicated for 10 h to achieve a homogenous dispersion, and then the sodium polysulfide (Na_2S_x) solution and 5 mM L^{-1}

* Corresponding author. Tel.: +1 510 486 5028; fax: +1 510 486 7303.
E-mail address: ejcairns@lbl.gov (E.J. Cairns).
[1] Visiting researcher from College of Materials Science and Engineering, South China University of Technology, Guangzhou 510641, PR China (Supervisor: Prof. Weishan Li).

0378-7753/$ – see front matter © 2012 Elsevier B.V. All rights reserved.
doi:10.1016/j.jpowsour.2012.01.047

surfactant hexadecyl trimethyl ammonium bromide (CTAB) were added and sonicated for 2 h to prepare Solution (I). Solution (I) was titrated into 100 ml of 2 mol L^{-1} formic acid solution (HCOOH) at a rate of 30–40 drops min^{-1} with stirring for 2 h. After reaction, the resulting suspension was filtered, then repeatedly rinsed with acetone and distilled water to remove surfactant. Finally, the precipitate was dried in vacuum at 50 °C for 24 h. The reaction formula is as follows:

$$S_x^{2-} + 2H^+ \rightarrow (x-1)S + H_2S$$

2.2. Preparation of the C–S cathode

The C–S electrode was prepared from a mixture of 80 wt.% of C–S composite, 8 wt.% of carbon nano-fibers, 2 wt.% of carbon particles, 10 wt.% of binder carboxy methyl cellulose (CMC) and styrene butadiene rubber (SBR) (CMC:SBR = 2:3, by weight). Water served as dispersant. The resulting slurry was coated onto a carbon-coated Al foil substrate using a doctor blade. The solvent was allowed to evaporate overnight at ambient temperature. The resulting cathode film (ca. 50 μm thick) was used to prepare the cathodes by punching circular discs having an area of 0.9 cm^2. These discs were dried at 50 °C under vacuum for 48 h before use.

For comparison, a mixture of 80 wt.% of C–S composite, 10 wt.% of carbon particles, 10 wt.% of CMC + SBR (CMC:SBR = 2:3, by weight) was prepared. 1 M kg^{-1} LiTFSI in PYR_{14}TFSI + PEGDME (PYR_{14}TFSI: PEGDME = 1:1, by weight) was used as liquid electrolyte [13]. N-methy-N-butylpyrrolidinium bis(trifluoromethanesulfonyl)imide (PYR_{14}TFSI), poly(ethylene glycol) dimethy ether (PEGDME, M_w = 250) and lithium bis(trifluoromethylsulfonyl) imide (LiTFSI) were purchased from Aldrich–Sigma and used without further treatment.

2.3. Characterization and measurements

The morphology of the samples was investigated using a scanning electron microscope (SEM-JEOL JSM 7500F). The sulfur content of the composite was ascertained by thermogravimetric analysis (NETZSCH STA 409 PC/PG). CR2032-type coin cells were assembled, using lithium foil as the negative electrodes, Cellgard 2400 microporous membrane as separator and 1 M kg^{-1} LiTFSI in PYR_{14}TFSI + PEGDME (PYR_{14}TFSI: PEGDME = 1:1, by weight) as the electrolyte. The cells were assembled in an Argon-filled glove box.

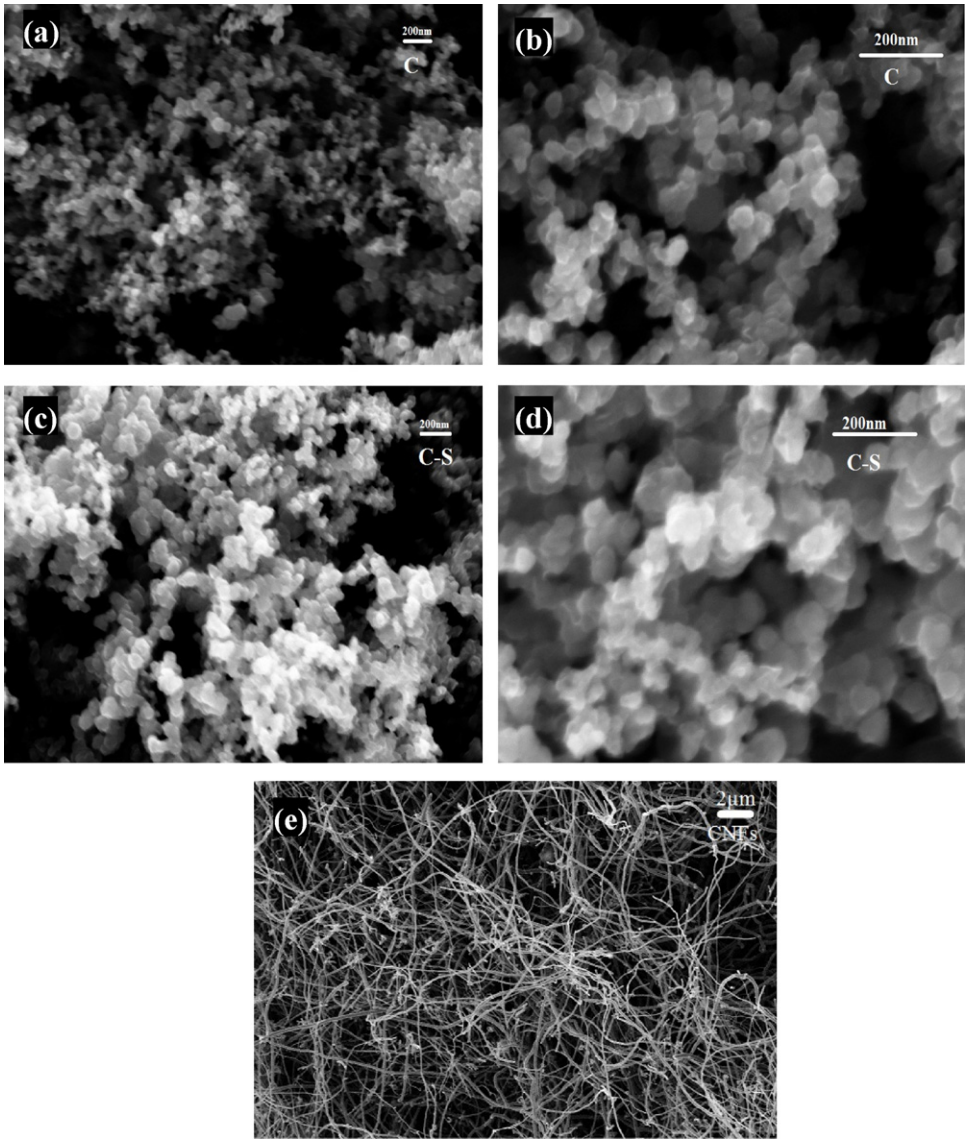

Fig. 1. SEM images of carbon particles (a) and (b), C–S composites (c) and (d), and electrical conductor CNFs (e).

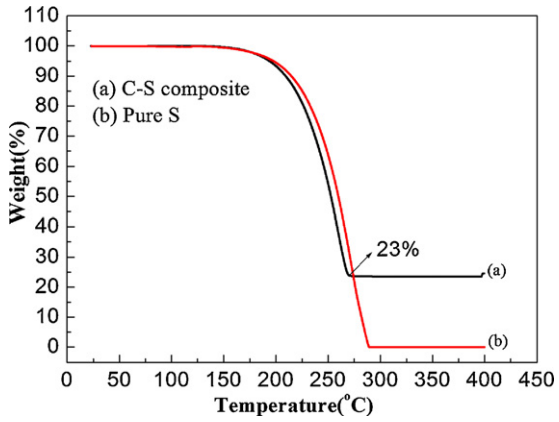

Fig. 2. TGA curves for the C–S composite (a) and pure sulfur (b) from room temperature to 400 °C at a heating rate of 5 °C min^{-1} under a N_2 atmosphere.

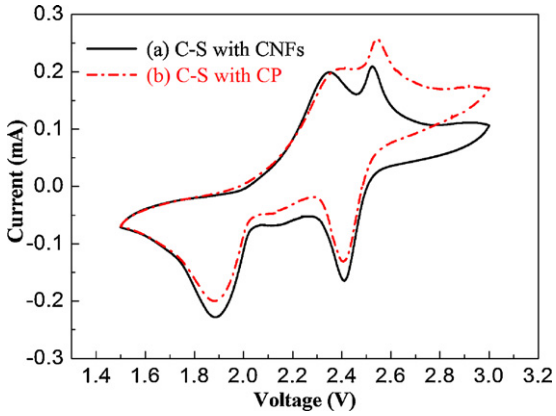

Fig. 3. Cyclic voltammograms of the lithium/sulfur cells with C–S cathode with CNFs (a) and C–S cathode with CP (b), at scan range: 3.0–1.5 V; scan rate: 0.05 mV s^{-1}.

EIS measurements of the cells were implemented with the use of a Solartron 1480. The impedance spectroscopy sweeps were conducted from 10 kHz to 100 mHz at an amplitude of ±5 mV. The discharge–charge tests were carried out with a Maccor cycle life tester with the voltage range 1.5–3.0 V. The specific capacity was calculated on the basis of the active sulfur material. Cyclic voltammetry (CV) experiments were conducted using Solartron 1480 at a scan rate of 0.05 mV s^{-1}.

3. Results and discussion

3.1. SEM of carbon–sulfur composite material

Fig. 1 shows the morphological characterization of the carbon particles, the C–S composite and the electrical conductor CNFs. The carbon particles have an average particle size of about 30 nm (Fig. 1a and b). The particles of C–S composite which was prepared by the chemical deposition method are a little larger than the carbon particles, and the average particle size is 50 nm (Fig. 1c and d), which means that the sulfur layer is about 10 nm thick. While the sodium polysulfide (Na_2S_x) solution with carbon particles was titrated into the formic acid solution, the polysulfide on the surface of the carbon particles reacted with the formic acid to form a deposit of sulfur on the carbon surface. The sulfur deposit then grows to wrap the whole carbon particle. Fig. 1(e) shows a SEM image of the CNFs used as electrical conductor. The CNFs have a network-like structure, which is expected to provide good electrical connection and structural stability for the sulfur electrode.

3.2. TGA analysis

The sulfur content of the C–S composite was ascertained by thermogravimetric analysis, under a N_2 atmosphere, from room temperature to 400 °C at a heating rate of 5 °C min^{-1}. Fig. 2 shows the TGA results obtained from the as prepared C–S composite and pure sulfur. It can be seen from Fig. 2(a) that the weight of the C–S composite decreases as the temperature increases from 150 °C and the weight loss is continuous until the C–S is heated to over 280 °C, which indicates that the reduction in weight of the C–S composite is due to evaporation of sulfur. The sulfur content was 77% in the C–S composite. The attribution of the weight loss to the evaporation of the sulfur in the C–S composite is also confirmed by the TGA curve of pure sulfur, as shown in Fig. 2(b). The sulfur content of this composite is higher than that of other C–S composites recently reported.

3.3. Cyclic voltammogram

Fig. 3 shows cyclic voltammograms of Li/S cells at a scan rate of 0.05 mV s^{-1}. It can be seen from Fig. 3 that both the CV curves of the sulfur cathodes with CPs and CNFs as conductor show two oxidation and reduction peaks. The 2.4 V reduction peaks are related to the change from elemental sulfur to the higher-order lithium polysulfides (Li_2S_n, $n \geq 4$); the reduction peaks between 1.8 V and 2.0 V are related to the reduction of higher-order lithium polysulfides to lower-order lithium polysulfides (Li_2S_n, $n < 4$) and lithium sulfide. [7,12,23]. The narrow current peak at 2.4 V of the cathodic sweep indicates that the sulfur composite has rapid kinetics. The offset from the anodic peak is relatively small. In contrast, the lower-potential peaks are broader and have a larger offset, indicating slower kinetics for the reaction involving Li_2S. The two reduction peaks in Fig. 3 correspond to the two discharge plateaus shown in Fig. 4. Compare the peaks of the two cathodes: the reduction and oxidation peaks of the C–S cathode with CNFs are sharper and show smaller offset than those of the C–S cathode with CP. The CV results indicate that the polarization of the C–S cathode with CP is larger than that of the C–S cathode with CNFs.

3.4. Cell performance

The first-cycle discharge–charge curves of the sulfur cathodes with CNFs and CP at room temperature are shown in Fig. 4. The discharge–charge capacity of the sulfur electrode with CNFs is

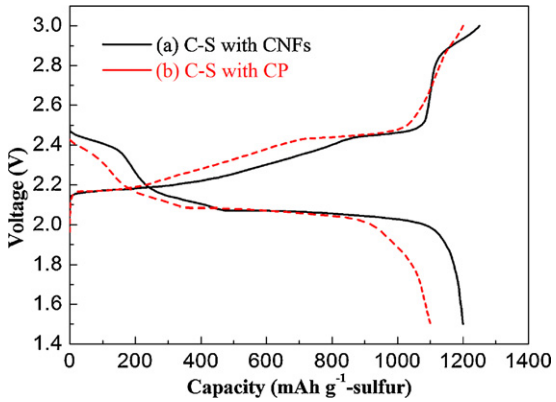

Fig. 4. The initial discharge and charge curves of lithium–sulfur cells: (a) C–S electrode with CNFs; (b) C–S electrode with CP, in LiTFSI (1 M kg^{-1}) + PYR_{14}TFSI + PEGDME (PYR_{14}TFSI: PEGDME = 1:1, by weight), discharge–charge rate: 0.05 C (C = 1645 mAh g^{-1}).

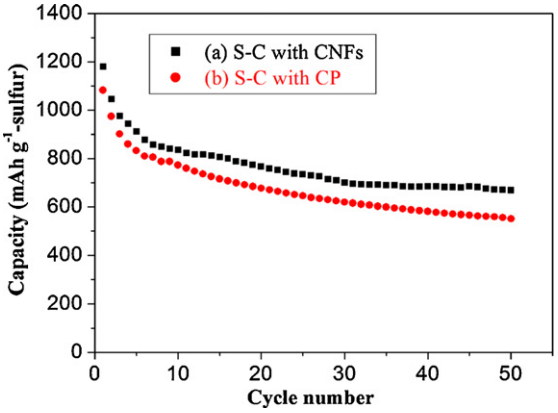

Fig. 5. The cyclability of a lithium/sulfur cell for 50 cycles: (a) C–S cathode with CNFs, (b) C–S cathode with CP, in LiTFSI (1 M kg^{-1}) + $PYR_{14}TFSI$ + PEGDME ($PYR_{14}TFSI$: PEGDME = 1:1, by weight), discharge–charge rate: 0.05 *C* (*C* = 1645 mAh g^{-1}).

larger than that of the electrode with CP's. The discharge curve shows two distinct plateaus at about 2.4 V (short upper plateau) and 2.1 V (long lower plateau), which is in accordance with the CV results, as shown in Fig. 3. It is found in Fig. 4 that the C–S cathode with CNFs shows an initial discharge capacity of 72% of the sulfur theoretical capacity, or 1200 mAh g^{-1}, whereas the C–S cathode with CP's only shows an initial discharge capacity of 66% of the sulfur theoretical capacity, or 1100 mAh g^{-1}. The improvement of the initial discharge capacity of the lithium/sulfur cell can be attributed to the improved conductivity with CNFs. Consequently, these results imply that the C–S cathode with CNFs has a good electrical network, and lithium ions can easily move into the sulfur electrode due to the high penetration of the electrolyte into the porous electrode structure [19,20].

Fig. 5 shows the cycling behavior of lithium/sulfur cells with C–S cathodes with CNFs and CPs for 50 cycles at 0.05 C. Both C–S electrodes show capacity loss with continued cycling, but the capacity loss rate is lower for the electrode with CNFs, especially at higher cycle numbers. After the first discharge, the discharge capacity of the C–S electrodes rapidly decreased until the 5th cycle. However, in subsequent cycles, the discharge capacity loss was less for the electrode containing CNFs. It can be seen from Fig. 5 that the C–S electrode with CNFs shows more stable capacity up to the 50th cycle, retaining about 668 mAh g^{-1} or 40% of the sulfur theoretical capacity, whereas for the C–S electrode with CP, the electrode retains only 550 mAh g^{-1} or 33% of the theoretical capacity. From this result it can be concluded that using CNFs as an electric conductor for the sulfur electrode provides a benefit in maintaining the capacity of the Li/S cell. In the case of the C–S electrode with CPs, the capacity decreases more rapidly than that with CNFs because of the agglomeration of sulfur (or lithium sulfide) during discharge/charge, as shown in Fig. 7(c).

3.5. Electrochemical impedance spectroscopy

Fig. 6 shows typical Nyquist plots of C–S cathodes with CPs and CNFs before discharge and after the 50th discharge. It can be seen from Fig. 6 that the Nyquist plots of C–S cathodes with CPs and CNFs before discharge are composed of a semicircle at high frequencies, which is related to the ohmic resistance and charge transfer resistance, and a short inclined line in the low frequency region, which is due to diffusion within the cathode [23,24]. Before discharge, the C–S cathode with CPs shows a higher charge-transfer resistance (R_{ct}) than the C–S cathode with CNFs. This is further evidence of the higher conductivity of the C–S cathode with CNFs.

After 50 cycles, there are two obvious semicircles in Fig. 6. Similar results were also discussed in Refs. [25,26]. The semicircle at high frequencies is related to the resistance and capacitance of the solid-state interface layer formed on the surface of the electrodes, the semicircle at medium frequencies is related to faradic charge-transfer resistance and its double-layer capacitance. It can be seen from Fig. 6 that the charge-transfer resistance of the C–S cathode with CNFs is smaller than that of the electrode with CPs. This can be explained by the fact that C–S cathode with CNFs has a better electrical path and more pores in the network-like structure than the C–S electrode with CPs, as shown in Fig. 7. Therefore, the movement of Li^+ to the electroactive sulfur is easier for C–S cathode with CNFs. As for the increases in the charge transfer resistance of the C–S electrode with CP after the 50th discharge, the main reason may be the poor electrical contact caused by severe morphology change of the sulfur cathode, as shown in Fig. 7(c). The addition of CNFs could improve the interfacial property between the electrodes and electrolyte, which led to a lower charge transfer resistance. The results suggest that CNFs were more critical to the improvement of the electrochemical performance of lithium/sulfur cells.

3.6. Morphological changes of the cathodes

Fig. 7 shows the SEM images of the C–S electrodes with CP and CNFs before and after 50 cycles. It can be seen from Fig. 7(b) that the C–S composites are well-distributed in the C–S electrode with the CNFs, and the core–shell structure of the C–S composites ensures the contact area between the sulfur and carbon. After 50 cycles, the C–S cathode with CNFs still displays a homogeneous distribution of C–S composites as shown in Fig. 7(d). As to the C–S cathode with CP conductor, although a well-distributed morphology was observed before discharge as shown in Fig. 7(a), aggregation of sulfur or lithium sulfide appears after 50 cycles, as shown in Fig. 7(c). In this case, the resistance of the C–S electrode with CPs increases as shown in Fig. 6 due to the partial loss of electrical contact and

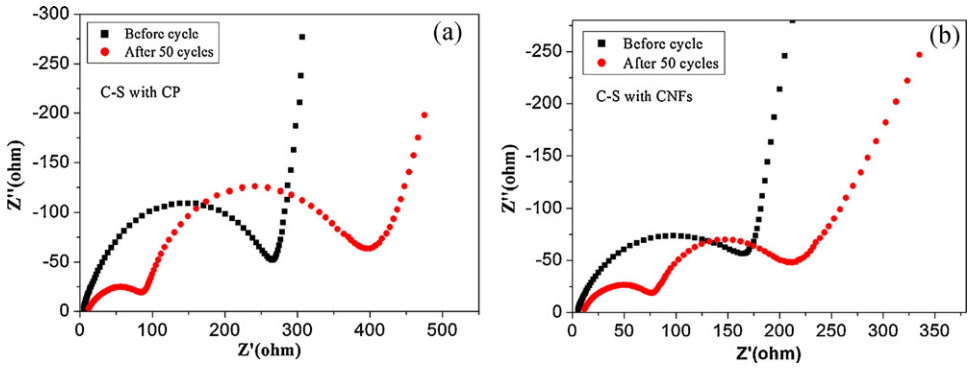

Fig. 6. The impedance plots of lithium/sulfur battery with C–S cathode with CP (a) and C–S cathode with CNFs (b), frequency range: 100 kHz to 10 mHz.

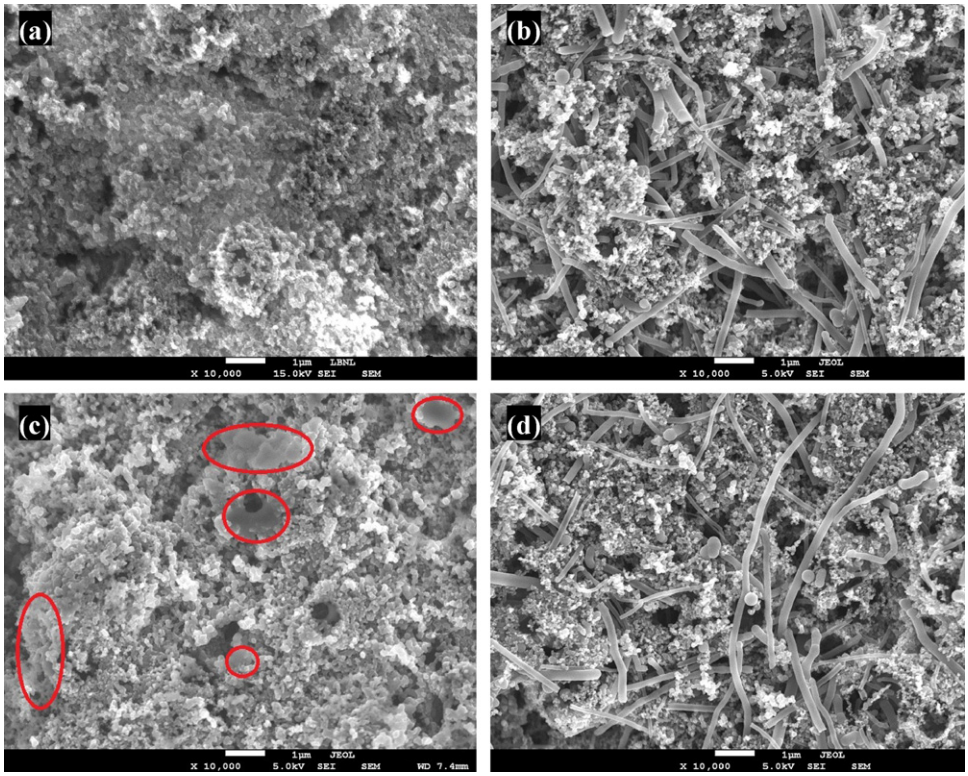

Fig. 7. SEM images of C–S electrodes with (a) CP and (b) CNFs before discharge; (c) CP and (d) CNFs after 50 cycles.

eventually, the discharge capacity decreases as shown in Fig. 5. The SEM results suggest that the capacity fading for the composite sulfur cathodes is mainly due to the heterogeneity of the cathode's morphology, which could worsen the distribution of sulfur or lithium sulfide as a result of cycling, and a C–S electrode with well dispersed CNFs can suppress the agglomeration of sulfur or lithium sulfide which may be attributed to the electrical path provided by the network-like structure provided by the CNFs. These results are in good agreement with the results from the electrochemical measurements.

4. Conclusions

A carbon particle supported sulfur composite cathode material was prepared by a simple chemical deposition method. Sulfur is chemically deposited to provide a nano-scale sulfur deposit that is dispersed uniformly on the carbon particle conductor. We investigated the effects of CNFs as electronic conductor by addition to the sulfur electrode. The cycling behavior was improved when CNFs were added to the sulfur electrode because the CNFs provide a good conductive network with structural stability. The C–S electrode with CNFs showed more stable cycling up to at least the 50th cycle due to the suppression of agglomeration of sulfur or lithium sulfide. The high retention of the polysulfides in the cathodes based on CNFs would also contribute to high sulfur utilization. The unique structure of the sulfur electrode with CNFs is important for potential practical applications, indicating that the combination of the C–S nanocomposite and CNFs is a promising candidate cathode material for high-performance lithium/sulfur cells.

Acknowledgments

M.R. was partially supported by the China Scholarship Council while visiting the Department of Chemical & Biomolecular Engineering at UC Berkeley.

References

[1] E.J. Cairns, P. Albertus, Annu. Rev. Chem. Biomol. Eng. 1 (2010) 299–320.
[2] R. Marom, S.F. Amalraj, N. Leifer, D. Jacob, D. Aurbach, J. Mater. Chem. 21 (2011) 9938–9954.
[3] B. Scrosati, J. Hassoun, Y.K. Sun, Energy Environ. Sci. 4 (2011) 3287–3295.
[4] M.M. Rao, J.S. Liu, W.S. Li, Y.H. Liao, Y. Liang, L.Z. Zhao, J. Solid State Electrochem. 14 (2010) 255–261.
[5] X. Ji, L.F. Nazar, J. Mater. Chem. 20 (2010) 9821–9826.
[6] X. Ji, K.T. Lee, L.F. Nazar, Nat. Mater. 8 (2009) 500–506.
[7] Y. Cao, X. Li, I.A. Aksay, J. Lemmon, Z. Nie, Z. Yang, J. Liu, Phys. Chem. Chem. Phys. 13 (2011) 7660–7665.
[8] S. Li, M. Xie, J. Liu, H. Wang, H. Yan, Electrochem. Solid-State Lett. 14 (2011) A105–A107.
[9] N. Jayaprakash, J. Shen, S.S. Moganty, Angew. Chem. Int. Ed. 50 (2011) 5904–5908.
[10] H. Wang, Y. Yang, Y. Liang, J.T. Robinson, Y. Li, A. Jackson, Y. Cui, H. Dai, Nano Lett. 11 (2011) 2644–2647.
[11] D. Marmorstein, T.H. Yu, K.A. Striebel, F.R. McLarnon, J. Hou, E.J. Cairns, J. Power Sources 89 (2000) 219–226.
[12] J. Shim, K.A. Striebel, E.J. Cairns, J. Electrochem. Soc. 149 (2002) A1321–A1325.
[13] J.H. Shin, E.J. Cairns, J. Power Sources 177 (2008) 537–545.
[14] J.H. Shin, E.J. Cairns, J. Electrochem. Soc. 155 (2008) A368–A373.
[15] C. Wang, J. Chen, Y. Shi, M. Zheng, Q. Dong, Electrochim. Acta 55 (2010) 7010–7015.
[16] J. Chen, X. Jia, Q. She, C. Wang, Q. Zhang, M. Zheng, Q. Dong, Electrochim. Acta 55 (2010) 8062–8066.
[17] S. Wei, H. Zhang, Y. Huang, W. Wang, Y. Xia, Z. Yu, Energy Environ. Sci. 4 (2011) 736–740.
[18] J. Wang, S.Y. Chew, Z.W. Zhao, S. Ashraf, D. Wexler, J. Chen, S.H. Ng, S.L. Chou, H.K. Liu, Carbon 46 (2008) 229–235.
[19] W. Zheng, Y.W. Liu, X.G. Hu, C.F. Zhang, Electrochim. Acta 51 (2006) 1330–1335.
[20] Y. Choi, K.W. Kim, H.J. Ahn, J.H. Ahn, J. Alloys Compd. 449 (2008) 313–316.
[21] L. Ji, M. Rao, H. Zheng, L. Zhang, Y. Li, W. Duan, J. Guo, E.J. Cairns, Y. Zhang, J. Am. Chem. Soc. 133 (2011) 18522–18525.
[22] L. Ji, M. Rao, S. Aloni, L. Wang, E.J. Cairns, Y. Zhang, Energy Environ. Sci. 4 (2011) 5053–5059.
[23] Y.J. Choi, Y.D. Chung, C.Y. Baek, K.W. Kima, H.J. Ahn, J.H. Ahn, J. Power Sources 184 (2008) 548–552.
[24] S.R. Narayanan, D.H. Shen, S. Surampudi, A.I. Atta, G. Halpert, J. Electrochem. Soc. 140 (1993) 1854–1861.
[25] W. Wang, Y. Wang, Y. Huang, C. Huang, Z. Yu, H. Zhang, A. Wang, K. Yuan, J. Appl. Electrochem. 40 (2010) 321–325.
[26] B. Zhang, X. Qin, G.R. Li, X.P. Gao, Energy Environ. Sci. 3 (2010) 1531–1537.